Investigation of speckle suppression beyond human eye sensitivity by using a passive multimode fiber and a multimode fiber bundle

ANATOLY LAPCHUK,[1,2] ZICHUN LE,[1,*] YANYU GUO,[1] YANXIN DAI,[1] ZONGSHEN LIU,[1] QIYONG XU,[1] ZHIYI LU,[1] ANDRIY KRYUCHYN,[2] AND IVAN GORBOV[2]

[1]*College of Science, Zhejiang University of Technology, Hangzhou 310023, China*
[2]*Institute for Information Recording of NAS of Ukraine, Shpak Str. 2, Kiev 03113, Ukraine*
[*]lzc@zjut.edu.cn

Abstract: A method of speckle suppression without any active device is expected for pico-projectors. The effectiveness of the passive method of speckle reduction using a single multimode fiber and a multimode fiber bundle was actually measured and theoretically analyzed. The dependences of the speckle contrast and speckle suppression coefficient on the parameters of multimode fiber and projection systems were investigated. Our results shown that the efficiency of speckle suppression was limited because only the radial direction of the objective lens aperture was used. An improvement using both of the radial and azimuthal directions of the objective lens aperture is required.

1.   Introduction

Lasers have wide applications due to their unique properties, including high beam quality, high brightness, narrow spectrum, ability to emit very short light pulses, and high optical efficiency [1–3]. Portable laser projectors are a popular application of lasers, because the high beam quality, high optical efficiency, and small waveband range of lasers can result in very small-sized projectors that can produce high-quality color saturated images [4–7]. However, currently, the use of laser pico-projectors poses a challenge, the main obstacle being laser speckles. When the screen is illuminated by a laser beam, the image of the light spot is strongly modulated by granular noise called subjective speckle [8]. The subjective speckle arises from the interference effect of light scattering from different areas of the screen in an image system. If the speckle noise is intense, a large speckle suppression effect is needed to obtain high-quality pictures. Speckle contrast C is used to estimate the level of speckle noise [8].

$$C = \sigma/\bar{I} \tag{1}$$

where $\bar{I}$ is the average intensity, and σ is the standard deviation of the light intensity of the image. Typically, single-mode lasers produce images with a speckle contrast close to 0.7. The human eye cannot distinguish speckle noise when the speckle contrast is below 0.03 [9]. Therefore, an efficient speckle suppression method, characterized by a speckle suppression coefficient of approximately 20, is required to obtain high-quality images. The speckle suppression coefficient k is defined as

$$k = C_0/C \tag{2}$$

where C_0 and C are the speckle contrast before and after applying the speckle suppression method, respectively. Most speckle suppression methods are based on speckle averaging by creating many decorrelated speckle patterns. It is well known that the image of a screen illuminated by N equal-intensity uncorrelated beams that produce uncorrelated speckle patterns has a speckle

contrast of $C = C_0/\sqrt{N}$. It is clear that approximately 400 uncorrelated speckle patterns are needed to obtain a speckle-free image.

Screen movement is a well-known method for decorrelating speckle patterns. However, accordingly, a shift for 400 decorrelated patterns during the time resolution of the human eye is needed to decrease the speckle noise to below human eye sensitivity [10–11]. Taking 1 mm as the eye resolution on the screen, a rather large shift speed (V) of 10 m/s (i.e., $400 \times 1 \times 25$ mm/s) is needed to obtain a speckle-free image. In addition, screen movement is not possible for many projector applications, and therefore, the above-mentioned solution is not technically preferable.

Speckle noise can also be decreased by reducing the coherence of the laser beam [8]. It is possible to decrease polarization and temporal or spatial coherence to obtain the speckle suppression effect [8,12]. Light has only two polarizations, and it can therefore produce two uncorrelated speckle patterns which, however, fall far short of the required quantity [12]. The wavelength bandwidth ($\Delta\lambda$) of efficient high-power lasers is not larger than 3 nm [13], and a wavelength shift at 1.5 nm is needed to obtain an uncorrelated speckle field. Hence, it is possible to obtain only three uncorrelated speckle fields by using a laser with the maximum possible temporal coherence decrease. However, this number is also far less than required.

Interestingly, spatial coherence functions differently. Since the eye has a small numerical aperture and the speckle correlation angle is determined by the size of this aperture, it is possible to use a large numerical objective lens aperture to decorrelate beams that pass through different parts of the objective aperture [8] and strongly decrease the speckle. It is possible to obtain many such decorrelated laser beams, and this number is approximately equal to the square of the ratio between the two numerical apertures, as follows:

$$N \sim (NA_{obj}/NA_{eye})^2 \tag{3}$$

where NA_{obj} and NA_{eye} are the numerical apertures of the objective lens and the pupil of the eye, respectively. Thus, it seems practical to obtain 400 decorrelated speckle patterns by using spatial laser beam decorrelation.

An active diffuser [14–15] or diffractive optical element (DOE) [16–21] can be inserted conjugate to the screen plane inside an optical system to decorrelate the beams that illuminate the screen at different angles. It is also possible to switch between DOE structures that produce uncorrelated speckle structures to obtain speckle noise averaging [17]. The general theory of the method based on an active DOE inside an optical system was explained in our previous research [22].

However, all these methods require mechanical displacement of the DOE or switching between different DOE structures to decorrelate beams. Mechanical movement is best avoided as a technical solution since it increases device complexity and volume, and is vulnerable to failure. On the other hand, fast switching (to approximately 10 kHz) between different DOE structures is still an unresolved problem. Thus, it is very important to find an efficient method for speckle reduction based on passive optical elements only.

It is possible to separate a laser beam into several sub-laser beams by using a DOE or a semitransparent mirror. Both use different optical paths for decorrelating, followed by the provision of beams incident on the screen under the decorrelated angles [23]. However, this method is difficult to realize for large values of N. Another solution involves using a light pipe or multimode fiber bundle to obtain sufficiently large speckle suppression [8,24–26]. An objective speckle arises at the far end of a light pipe or multimode fiber bundle due to the interference of a large number fields of waveguide modes [8,24]. It was shown that by using significantly long multimode fibers, it is possible to decorrelate the light of different waveguide modes due to the different speeds of propagation. Thus, it becomes possible to suppress objective speckles to a very low level. The theory for speckle contrast evaluation at the far end of a multimode fiber was developed [8,25]. For a laser with a radiation continuum spectrum of Δf, the speckle contrast can

be calculated by the formula

$$C(L) = \left(1 + 0.5\left(2\pi\Delta f\Delta t/\sqrt{3}\right)^2\right)^{-1/4}, \quad \Delta f = c\Delta\lambda/\lambda^2, \ \Delta t = L(NA)^2/(2nc) \tag{4}$$

where L, λ, and f stand for fiber length, laser radiation wavelength, and frequency, respectively; n and c are the fiber core refractive index and light speed, respectively; and $\Delta\lambda$, Δf, and Δt are the wavelength band, frequency band, and decorrelated time for the laser beams, respectively. It is not difficult to calculate that for a green laser with a wavelength band of 1 nm, it is sufficient to use a 7-m multimode fiber with a numerical aperture of 0.3 to obtain a speckle contrast below 3.5%. It was assumed that this method can be used to obtain a speckle-free laser image without any active optical device [25]. However, there is few experimental research to demonstrate its effectiveness.

In the present study, a speckle suppression method without active devices was investigated. A single multimode fiber of different lengths, a multimode fiber bundle with multiple fibers, and a combination of a multimode fiber bundle and a DOE were adopted for speckle suppression. Several experimental systems for laser projection were set up to measure the speckle contrast and the speckle suppression coefficient. Using the obtained experimental results, we analyzed and discussed the dependence of the efficiency of speckle contrast suppression on the optical parameters of the laser projector systems, especially those corresponding to the multimode fiber and multimode fiber bundle. To thoroughly understand the speckle characteristics, a theoretical model was developed to explain the experimental results. The theoretical prediction was found to be in good agreement with the experimental results. Moreover, as the theoretical model was developed for a general multimode optical waveguide, it is valid not only for multimode fibers, but also for other optical waveguides of different waveguide cross-section shapes.

2. Experimental setup

To evaluate speckle suppression efficiency using a multimode fiber in a laser projector, we should measure the speckle contrast in the image of the screen illuminated by the laser beams that pass through the fiber. The far end of the fiber should be placed in the optical plane conjugate to the screen to obtain an image of the fiber end on the screen. We used a single multimode optical fiber and a multimode fiber bundle in the experiments, whose optical schemes are shown in Figs. 1 and 2. In the experiment with a single multimode fiber (see Fig. 1), we used a fiber with a core diameter (d) of 1 mm and a numerical aperture (NA_f) of 0.37. In Figs. 1 and 2, S_1, S_2, S_3, S_4, and S_5 stand for the distance from the converging lens to the front end of fiber (fiber bundle), the distance from the back end of fiber (fiber bundle) to the objective lens, the distance from the objective lens to the screen, the distance from the screen to the camera lens, and the distance from the camera aperture to the photodiode array matrix, respectively. D_2, D_3, and D_4 stand for the aperture of camera lens, the aperture of the lens which converges light to the front end of fiber (fiber bundle), and the aperture of the objective lens, respectively. We measured the speckle suppression effect for the fiber lengths (L) of 2, 4, 7, 10, and 15 m. The input beam should excite the multimode regime to allow multiple propagation modes for speckle suppression. The numerical aperture of the input beam in this case excites the waveguide modes that propagate in a cone angle corresponding to the numerical aperture of the incident beam. We changed the diameter of the diaphragm aperture D_1 to excite the propagation modes in different numerical aperture ranges. The relatively small distance from the fiber back end to the objective lens results in a change in the area of the objective lens, which is filled with light, and therefore changes the numerical aperture of the incident beam on the screen. It should be noted that due to the unideal ends of the fiber and the fact that the fiber is twisted in rings of a diameter of approximately 300 mm, the output numerical aperture can differ from the input numerical aperture of the beam for a fiber. Therefore, we also measure the numerical aperture of the output beam from the fiber.
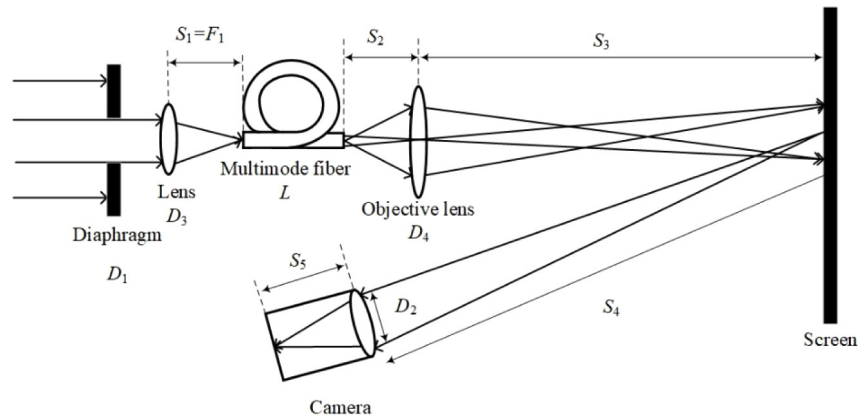
Fig. 1. Optical scheme for measuring the speckle suppression efficiency using a single multimode optical fiber with different fiber lengths L and different diaphragm diameters (D_1). $S_1 = 45$ mm, $S_2 = 62$ mm, $S_3 = 1810$ mm, $S_4 = 1580$ mm, $S_5 = 25$ mm, and $D_2 = 1$ mm.
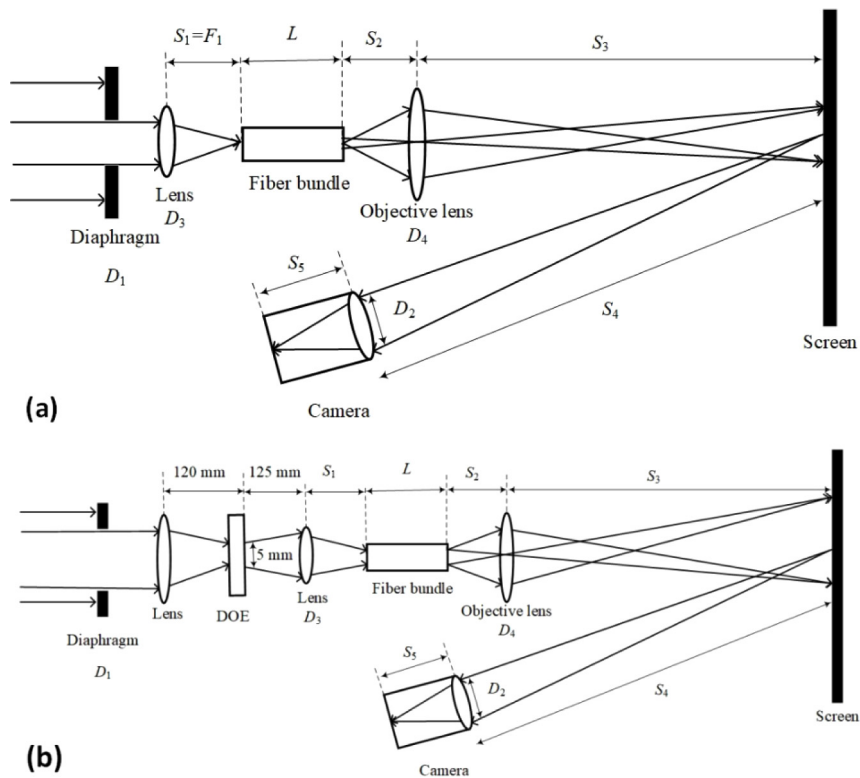

(a)

(b)

Fig. 2. Optical scheme for speckle suppression efficiency measurement by a multimode fiber bundle with $L = 400$ mm, $S_1 = 125$ mm, $S_2 = 62$ mm, $S_3 = 1500$ mm, $S_4 = 1600$ mm, $S_5 = 25$ mm, $D_1 = 25$ mm, $D_2 = 1$ mm, $D_3 = 25$ mm, and $D_4 = 51$ mm. (a) Fiber bundle excited by a quasi-collimated laser beam, and (b) every fiber in the bundle excited by a cone of diffracted beams from the 2D DOE based on the Barker code with code length $M = 13$.

For the short fiber ($L = 400$ mm), we also use a fiber bundle with a regular hexagon shape and tightly packed fibers without gaps. The diameter of each fiber is 25 μm with a numerical aperture NA_f of 0.25, and the total bundle diameter is 5 mm. The experimental setup for this case is shown in Fig. 2(a). The size of the light beam is decreased to the size of the fiber bundle by a lens. Since the laser spot is many times larger than that in the case of a single fiber, the input light for every fiber within the bundle is a quasi-collimated laser beam with little change in the incident angle from fiber to fiber, in accordance with the ray propagation direction of the converging beam focused by the first lens.

We use the third optical scheme shown in Fig. 2(b) to excite the multimode regime in every fiber within the fiber bundle. The collimated laser beam is refracted by the first lens and then scattered by the DOE on the transparent plate before it illuminates the fiber bundle. The DOE breaks up the converging beam into a cone of divergent beams. The second lens creates an image of the DOE at the front end of fiber bundle. The light that passes through the DOE excites a wide spectrum of modes in every fiber within the fiber bundle due to the diffraction orders of the spectrum fields. A 2D DOE structure based on the Barker code with a code length (M) of 13 is used in our experiments to excite a large number of diffraction orders. The DOE has an elementary cell size (T) of 6 μm and a period size of 78 μm. The width of the beam divergence after the DOE can be estimated as $\sin\theta = \lambda/T$, and therefore, the mode spectrum in optical fiber should be excited in the same range of the numerical aperture.

In both optical schemes shown in Fig. 2, the objective lens creates an image of the far end of the fiber on the screen. A camera is used to capture the picture of the light spot on the screen to evaluate the speckle level.

We use a green laser diode (LD, PL 520B1) and a blue laser diode (PL 450B) from OSRAM as sources of coherent illumination in the experiments. The radiation spectrums of the green and blue LDs are shown in Fig. 3. It is clear that the full spectrum ranges of both diodes are of a similar width, approximately 2 nm. However, the spectrum of the green LD is slightly wider than that of the blue LD.
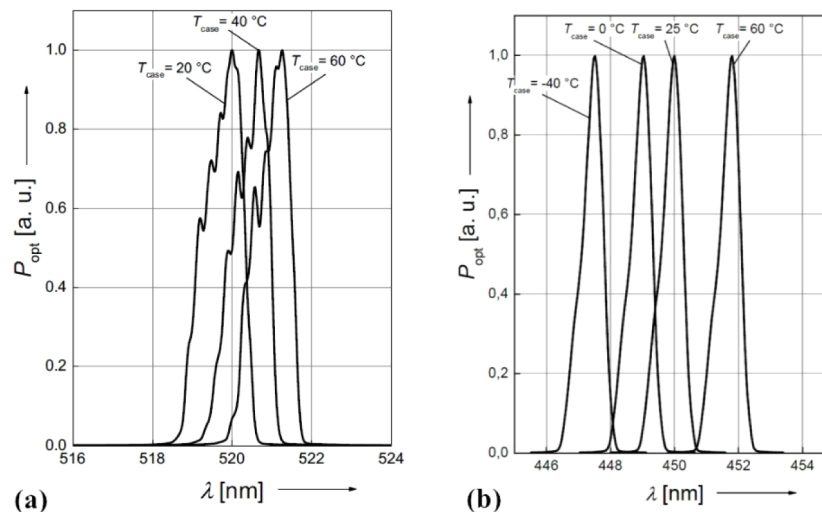

Fig. 3. Radiation spectrums of the lasers used in the experiments with the (a) green LD (PL 520B1) and (b) blue LD (PL 450B).

It should be noted that the laser diodes do not have a stabilization driving circuit, and we do not use vibration isolation in our experiments. Therefore, the speckle contrast measurement shows slow variation in terms of time (approximately ± 20%). Since the light spot is small due

to the small fiber cross-section, we produce five photos of light spots on different places on the screen (using screen shifting) to test the statistical averages for more accurate speckle contrast evaluation.

3. Experimental results and discussions

The dependence of the speckle contrast on the multimode fiber length for the green and blue LDs is shown in Fig. 4 for different input beam apertures (NA_{in}). The speckle contrast for the green LD (Fig. 4(a)) decreases rapidly with the increase in the numerical aperture at first, and then, it reaches saturation when the fiber length exceeds 7 m. The speckle contrast decreases faster for larger numerical apertures and smaller fiber lengths, which is in good agreement with the theoretical results reported in [25]. The experiment reaches saturation faster with the increase in the fiber length for large NA_{in}, and larger NA_{in} values provide a higher speckle suppression effect. The speckle contrast for the blue LD (see Fig. 4(b)) shows similar performance; however, the speckle contrast decreases more slowly with the increase in the fiber length, and the saturation occurs later. This can be well explained by the fact that the blue LD has a narrower radiation waveband.
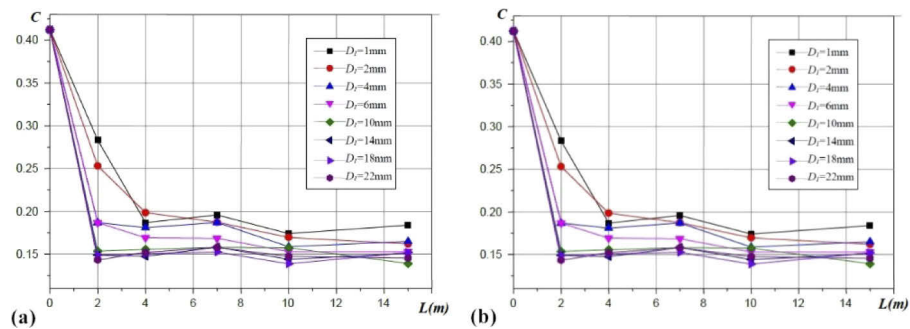

Fig. 4. Dependence of speckle contrast of the image on the screen on the fiber length for different diameters of aperture D_1 using the optical scheme shown in Fig. 1 for (a) the green LD and (b) the blue LD.
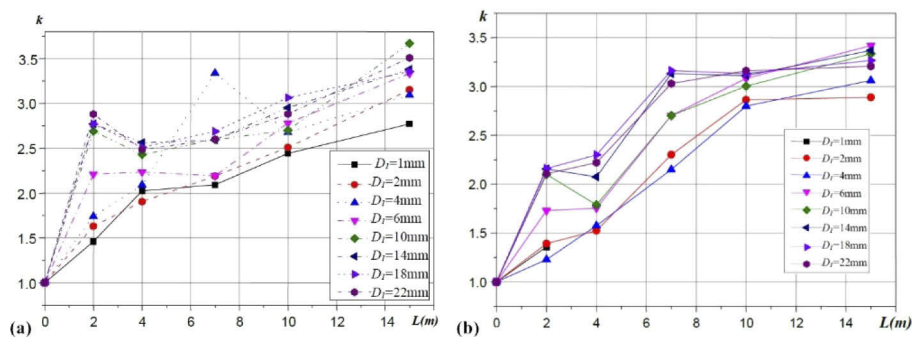

Fig. 5. Dependence of speckle suppression coefficient of the image on the screen on the fiber length for different diameters of aperture D_1 using the optical scheme shown in Fig. 1 for (a) the green LD and (b) the blue LD.

It should be noted that even for large fiber lengths ($L = 15$ m), the speckle contrast is large, and it appears as if one should not expect a large gain in speckle suppression effect with further increase in the fiber length due to the saturation.

Figure 5 shows the dependence of the speckle suppression coefficient k on the fiber length for the green LD (see Fig. 5(a)) and the blue LD (see Fig. 5(b)). The speckle suppression coefficient rises rapidly with the increase in the fiber length and reaches saturation for a large fiber length. The speckle contrast coefficient is larger for higher NA_{in} when the fiber length is small. However, it is almost the same for large fiber lengths. In spite of the large fiber length, the speckle suppression coefficient k does not exceed 3.5.

Figure 6 shows the dependence of the speckle contrast on NA_{in} for different fiber lengths. The speckle contrast decreases rapidly with the increase in the numerical aperture for small fiber lengths. For the green LD with large fiber lengths, we obtained practically the same speckle contrast, independent of NA_{in}. For the blue LD, the speckle contrast was significantly larger for two smaller values of NA_{in} ($D_1 = 1$ and 2 mm), even for large fiber lengths.
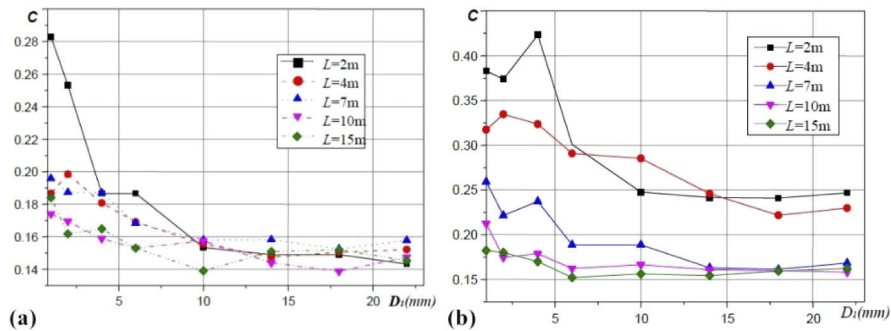

Fig. 6. Dependence of speckle contrast of the image on the screen on the diameter of the aperture D_1 (for different input numerical apertures) with different fiber lengths using the optical scheme shown in Fig. 1 for (a) the green LD and (b) the blue LD.

Figure 7 shows the dependence of speckle contrast C and speckle suppression coefficient k on NA_{in} for the blue LD with a fiber length 15 m when the distance from the camera to the screen is 200 mm (equivalent to a significant increase in the numerical aperture of the camera). Both parameters have similar dependences on NA_{in} for large distances to the camera (see Figs. 5 and 6). However, saturation is reached at higher speckle contrasts and smaller speckle suppression coefficients.
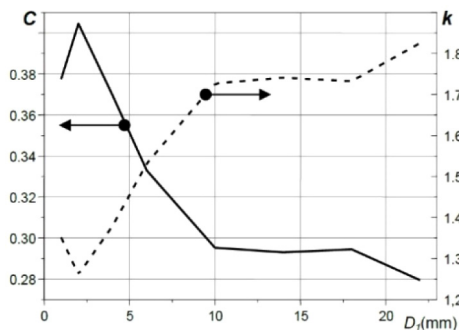

Fig. 7. Dependence of speckle contrast C (solid line) and speckle suppression coefficient k (dotted line) on the aperture D_1 for fiber length $L = 15$ m using the optical scheme in Fig. 1 for the blue LD, but the distance from the screen to the camera (S_4) is 200 mm.

For the fiber bundle of length 400 mm and without the DOE (see the optical scheme in Fig. 2(a)), we obtained values of 0.2 for C and 2.3–2.6 for k for the green LD, and corresponding

values of 0.3 and 1.86 for the blue LD. When using the DOE to excite the multimode regime in every fiber of the bundle (see the optical scheme in Fig. 2(b)), we obtained values of 0.17 and 3.27 for C and k, respectively, for the green LD and the corresponding values of 0.25 and 2.53 for the blue LD.

Figures 8 and 9 show the intensity distributions of the images on the screen for the green LD and blue LD, respectively, for different fiber lengths. From the presented intensity distributions, the speckle noise is obvious even when using a fiber as long as 15 m.
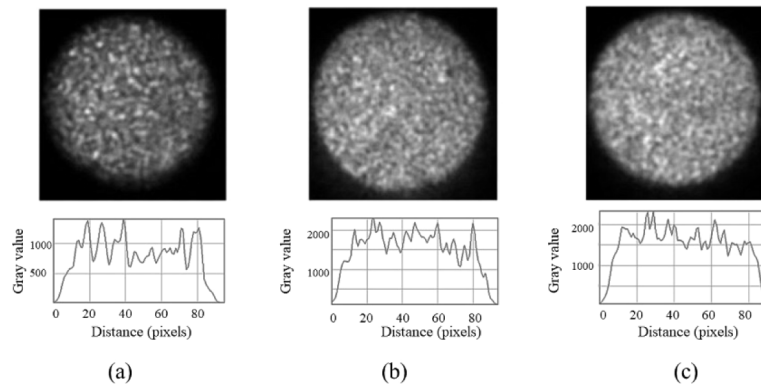

Fig. 8. 2D laser intensity distribution (upper panel) and 1D intensity distribution (lower panel) of the image on the screen with the green LD, (a) $L = 2$ m, $C = 0.150$; (b) $L = 4$ m, $C = 0.156$; (c) $L = 15$ m, $C = 0.139$. $D_1 = 10$ mm for all fiber lengths.
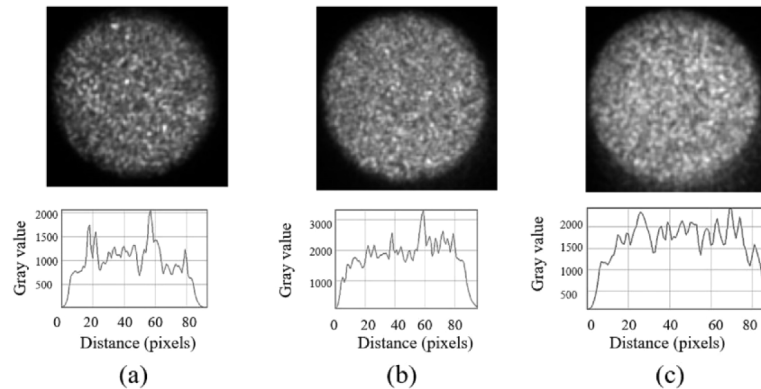

Fig. 9. 2D laser intensity distribution (upper panel) and 1D intensity distribution (lower panel) of the image on the screen with the blue LD, (a) $L = 2$ m, $C = 0.248$; (b) $L = 4$ m, $C = 0.285$; (c) $L = 15$ m, $C = 0.156$. $D_1 = 10$ mm for all fiber lengths.

Figure 10 shows the relation between the input numerical aperture NA_{in} and the output numerical aperture NA_{out} of the laser beam for different fiber lengths with the green LD (Fig. 10(a)) and blue LD (Fig. 10(b)). Figure 10 clarifies that during beam propagation along the fiber, the numerical aperture of the beam changes. The numerical aperture of the beam increases initially with the increase in fiber length. For an initially small NA_{in}, NA_{out} is always significantly larger than the initial value for all fiber lengths. The largest increase is noted for the fiber length of 4–7 m. Increase in the fiber length beyond this point results in a decrease in NA_{out}, especially for beams with large input numerical apertures. The change in the numerical aperture of the laser beams

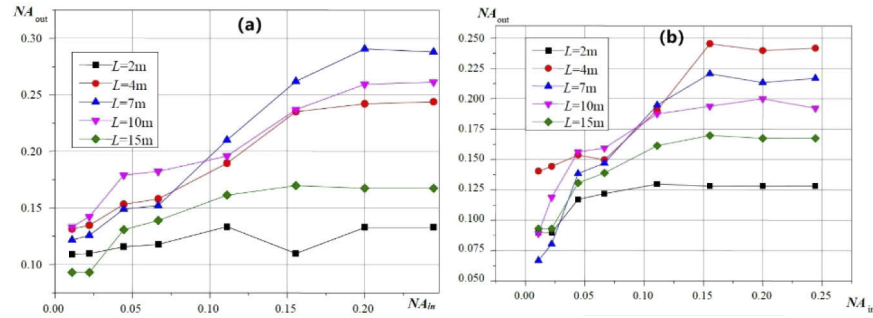denotes a transformation from one mode to another mode during the mode propagation in the multimode fiber.

Fig. 10. Dependence of output fiber beam aperture NA_{out} on the input fiber beam numerical aperture NA_{in} obtained during speckle suppression measurement.

Figure 11 shows the dependence of laser beam loss in the fiber for different initial apertures for a fiber length of 7 m for the green LD. The curve in Fig. 11 shows that after propagation along the fiber, higher modes propagating at a large angle to the fiber axis show large losses, resulting in the decrease of the numerical apertures of beams with large initial numerical apertures (see Fig. 10). Due to the mode transformation during propagation in the multimode fiber, the theory describing speckle statistical properties at the far end of the fiber needs to be amended.
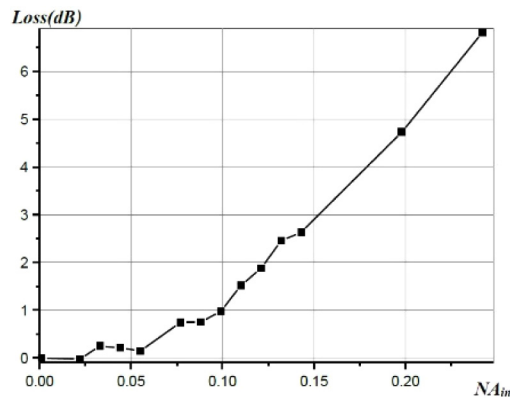

Fig. 11. Dependence of laser beam loss on input numerical aperture for a fiber length of 7 m for the green LD (calculated from image intensity).

4.   Theoretical model and explanation

The speckle in the image on the screen is a compound speckle since it is a superposition of the objective speckle due to mode interference and the subjective speckle due to light scattering on the screen. To highlight the objective speckle, we took photos of the light spot on a fast-moving screen when using a 15 m long fiber. Figure 12 shows the comparison of the photos of the moving and static screens for the green and blue LDs. The fast-moving screen strongly suppresses the subjective speckle, and the image is modulated only by the objective speckle. It is clear from Fig. 12(a) and 12(b) that the objective speckle at the far end of the fiber has a very low value of C (< 0.01), which is in full agreement with the theoretical prediction [25]. Thus, the mode transformation (transformation of one mode into another during propagation along the fiber) does

not noticeably influence the speckle suppression effect at the far end of the fiber. However, the speckle on the static screen is large and almost comprises the subjective speckle only. As per the obtained experimental results, speckle suppression on the static screen has a considerably low efficiency compared with that at the far end of a fiber. It is evident that the effect is not due to the small numerical aperture of the objective lens since the ratio of the apertures of the objective lens and camera lens is large ($NA_{out}/NA_{in} \approx 30$). This aspect can decrease the speckle to below 3% according to our previous analysis and as per [8]. Thus, a different principle applies for the speckle suppression mechanism at the far end of a fiber compared with that in the image on the screen illuminated by beams that have passed through the fiber.
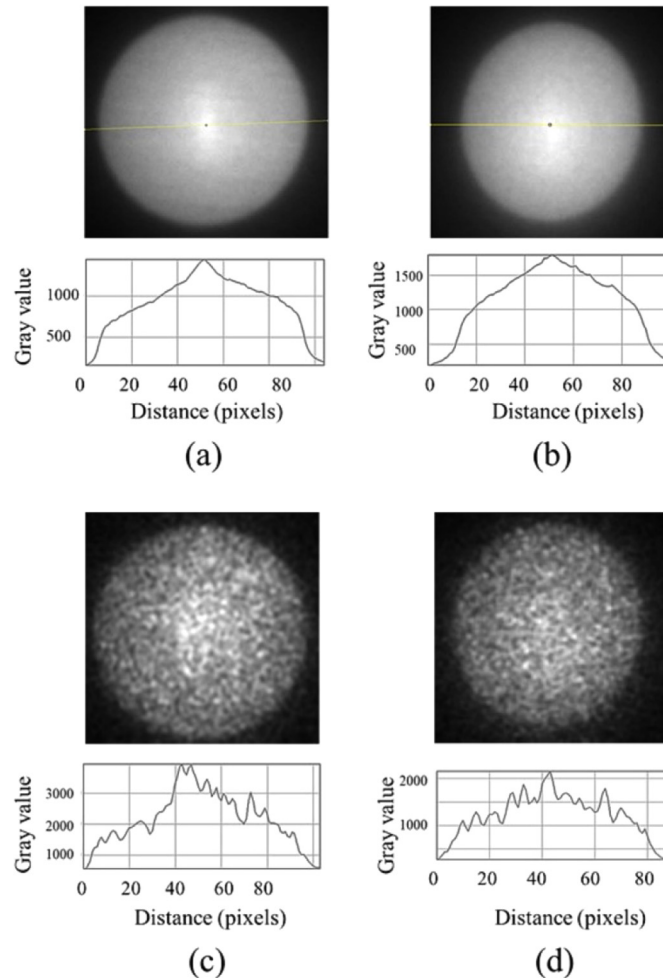

Fig. 12. Field intensity distributions for a fast-moving screen orthogonal to the optical axis ((a) and (b)) and for a static screen ((c) and (d)) for the green LD (left panel) and the blue LD (right panel) using the optical scheme shown in Fig. 1. (a) Green LD ($C < 0.01$); (b) Blue LD ($C < 0.01$); (c) Green LD ($C = 0.13$); (d) Blue LS ($C = 0.15$).

The speckle suppression at the fiber requires a decorrelation of the waveguide mode field at the end of the fiber; in other words, the difference in the optical paths between the two modes should be equal to or larger than the decorrelation length of the laser beam. To obtain the decorrelation of speckle patterns created by two beams for the image on the screen, a path difference larger than the decorrelation length of the laser beam is also required. Additionally, the laser beams

should propagate at an angle larger than the angular size of the camera aperture (diameter of the human eye's pupil) when seen from the screen. Therefore, to find the condition for speckle suppression in this case, we should identify the conditions of the modes involved to create the decorrelated speckle patterns.

We suppose that the waveguide is fabricated by a homogeneous dielectric with refractive index n and that the laser travels along the z-axis. The field of the regular waveguide mode can be written as follows:

$$\varphi(x, y, z) \sim f(x, y)\exp(-i\gamma z) \tag{5}$$

where x, y, and z stand for the axes in the Cartesian coordinate system, and $f(x,y)$ is the eigenfunction of differential equation $\frac{\partial^2 f(x,y)}{\partial x^2} + \frac{\partial^2 f(x,y)}{\partial y^2} = -k^2 f(x,y)$ with a special boundary condition, which depends on the type of waveguide. $\gamma_i = \sqrt{k^2 n^2 - (k_\perp^i)^2}$ is the wavenumber of the i-th mode, and $k_\perp^i$ is the transverse wavenumber of the i-th mode, which is an eigenvalue of the Laplace equation for a waveguide. The difference in the propagation speeds of these modes results in the decorrelation of the field of waveguide modes, which is defined by the dispersion of γ_i. According to the theorem in [27], the wavenumbers of the waveguide modes homogeneously fill in the 2D space of the wavenumbers, and the density of modes ($\rho(k_\perp)$) linearly increase with a rise in the transverse wavenumber ($k_\perp^i$); that is, $\rho(k_\perp) = \frac{dN(k_\perp^i)}{dk_\perp^i} : k_\perp^i$, where $N(k_\perp^i)$ is the number of modes with a transverse wavenumber smaller than $k_\perp^i$.

For the multimode waveguide with a circular cross-section (multimode fiber), the decorrelation areas, which depend on transverse wavenumbers, have cylindrical symmetry. The waveguide mode with transverse wavenumber $k_\perp^i$ radiates from the end of the fiber in the direction along angle θ (defined by $\sin\theta = k_\perp / k$), and almost all of the radiation intensity is concentrated within a small angle of $\Delta\theta = \lambda/(2a)$ around the cone surface, as shown in Fig. 14, where a is the radius of the multimode fiber. Therefore, the decorrelated modes radiate from the fiber end to create circular decorrelated areas (areas between the dashed circles, as shown in Fig. 13(a)) in the space of the transverse wavenumber. The red spot in Fig. 13 represents the camera aperture. The area between two red concentric circles tangential to the red spot is the decorrelated area that produces the decorrelated speckle pattern in the image on the screen taken by the camera (see Fig. 13(b)). We can calculate the amount of decorrelated speckle patterns (N) in the image on the screen as follows:

$$N = NA_{bm}/(2NA_{cm}) \tag{6}$$

where NA_{bm} and NA_{cm} are the numerical apertures of the beam from the fiber end and the camera, respectively. The intensity of radiation from the areas that produce decorrelated speckle patterns is proportional to their surface between the red circles in Fig. 13(b), and therefore, the intensity linearly increases with the distance to the objective aperture center (see Fig. 13(b)). Thus, the speckle contrast can be calculated approximately by a sum of N independent speckle patterns, and the intensity of each pattern linearly changes from 0 to the maximum value. The speckle suppression coefficient in the method based on using N uncorrelated speckle fields [25] can be calculated by

$$k = \sum_{i=1}^{N} I_i / \sqrt{\sum_{i=1}^{N} I_i^2} \tag{7}$$

where I_i is the intensity of the i-th speckle pattern. Using Eqs. (6) and (7) and the fact that the intensity of the laser beams producing uncorrelated speckle patterns increases linearly with the distance from the beam axis (considering the number of areas i, counting from the beam center; see Fig. 13(b)), it is easy to obtain the speckle suppression coefficient ($k = \sqrt{3 \cdot NA_{bm}/(4 \cdot 2NA_{cm})}$) for the method with the passive multimode fiber. Then, we can estimate the maximum speckle suppression coefficient using the fact that the maximum numerical aperture of the beam radiated

from the fiber end was approximately 0.28 and the camera aperture diameter was 1 mm. Therefore,

$$k = \sqrt{3NA_{bm}/(8NA_{cm})} = \sqrt{3 \cdot S_2 \cdot 0.28 \cdot 2 \cdot S_4/(8 \cdot D_2 \cdot S_3)} \approx 3.4 \qquad (8)$$

The theoretical estimation matches well with the experimental results (see Fig. 5). It should be noted that the theoretical estimation was obtained using only the assumptions that the optical waveguide is homogeneous dielectric and multimodal in nature; that is, its transverse size is considerably larger than the laser radiation wavelength. Therefore, this method should be valid for multimode waveguides with any cross-sectional shape.
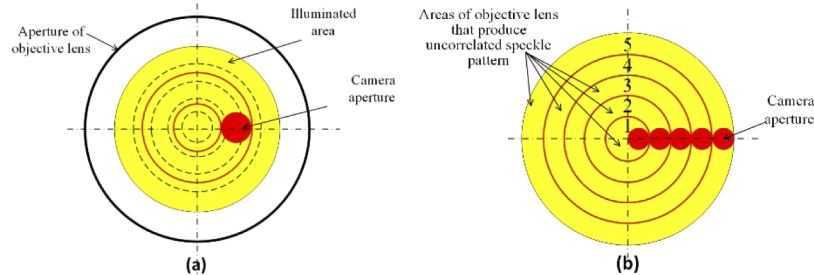

Fig. 13. Schematic diagram of the aperture of the objective lens, illuminated area, aperture of the camera, and decorrelated areas. (a) Aperture of the objective lens with the illuminated area (colored yellow), where the dashed circles separate decorrelated areas and the red spot denotes the aperture of the camera. (b) Illuminated aperture of the projector lens, aperture of the camera, and areas that produce decorrelated speckle patterns.
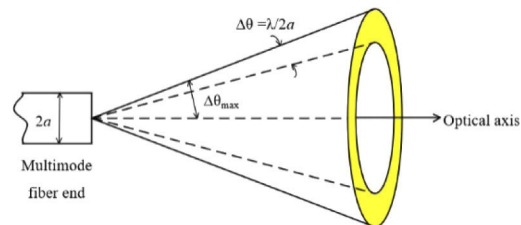

Fig. 14. Schematic diagram of the cone of radiation from the end of the fiber for high-order modes of the multimode fiber.

It is obvious that the current method used only the radial direction of the aperture of the objective lens to suppress the speckle. Thus, this is a 1D method and provides an effect similar to that obtained by using a 1D DOE to suppress the speckle [18]. Therefore, further increase in the fiber length will not provide a considerable speckle suppression effect. To obtain a considerably larger speckle suppression, a large increase in the objective lens aperture is needed. According to our theoretical analysis, a very large objective lens aperture (several hundred times larger than the numerical eye aperture) is needed to suppress the speckle to below that perceivable by the human eye, which is practically impossible to realize. Therefore, the method needs to be modified by using the azimuthal direction of the aperture to significantly improve the efficiency of speckle suppression.

In addition, we clarify some peculiarities of using fibers as multimode waveguides. According to the theory of scalar approximation fields, the modes propagating along the fiber in the z

direction can be presented in the cylindrical coordinate system as

$$\phi(\rho, \varphi, z) = \exp(-i\gamma_{mn}z)\exp(in\varphi)J_n(k_{\perp nm} \cdot \rho), \quad \rho < a \tag{9}$$

where $\rho = \sqrt{x^2 + y^2}$, $\varphi = \tan^{-1}(y/x)$, a is the radius of the fiber, and n and m denote the number of waveguide mode field oscillations in the azimuthal and radial direction, respectively. The amplitude of the spatial spectrum radiated from the far end of the fiber can be estimated (without taking into account the mode field disturbance at the fiber end, which is small for multimode fibers) as follows:

$$F(k_x, k_y) \sim \frac{a}{k_{\perp nm}^2 - k_\rho^2} \cdot 2\pi(i)^n \exp(in\varphi) \cdot [J_{n+1}(k_{\perp nm}a)J_n(k_\rho a) - J_n(k_{\perp nm}a)J_{n+1}(k_\rho a)] \tag{10}$$

and the resulting intensity of the spatial spectrum is

$$|F(k_x, k_y)|^2 \sim (2\pi)^2 \left|\int_0^a J_n(k_{\perp nm}\rho)J_n(k_\rho\rho)\rho d\rho\right|^2 = I(k_\rho) \tag{11}$$

where k_x and k_y are the x and y components of the wave vector of the laser radiation, respectively, and $k_\rho = \sqrt{k_x^2 + k_y^2}$. Then, the width of the radiation peak can be estimated by [28].

$$\int_0^a J_n(\alpha_m\rho)J_n(\alpha_l\rho)\rho d\rho = \begin{cases} 0, & m \neq l \\ \frac{1}{2}\rho^2 \left[\left(1 - \frac{n^2}{(\alpha_m\rho)^2}\right)J_n^2(\alpha_m\rho) + (J_n'(\alpha_m\rho))^2\right]\Big|_0^a \end{cases} \tag{12}$$

provided that α_m is a solution of equation $J_n(\alpha_m a) + bJ_n'(\alpha_m a) = 0$. Since the distance between the two adjacent solutions α_m and α_{m+1} is approximately equal to π/a, the radiation will lie between two close cones with a maximum angle of $\theta_{max} = \sin^{-1}(k_{\perp nm}/k)$ to the optical axis, and the angle between these two cones is $\Delta\theta = \lambda/(2a)$, as shown in Fig. 14.

The theoretical analysis for the modes' fields validates the general assumption made above. The radiation field patterns of the multimode waveguides used to derive Eq. (10) can be applied to estimate the speckle suppression coefficient of the method with passive multimode waveguides having arbitrary cross-sections.

5. Conclusions

A speckle suppression method without active devices was investigated. A single multimode fiber, a multimode fiber bundle, and a combination of a multimode fiber bundle and a DOE were used in our experiments for speckle suppression. The obtained experimental results were adequately analyzed and discussed, especially for single multimode fibers.

The experimental results obtained by using the passive multimode fiber showed that in spite of a considerably long fiber length of 15 m, the method was not sufficient for speckle-free laser projection. A theoretical model was developed for explaining the experimental results, and the theoretical analysis showed that the current method resulted in a circular area of decorrelation in the space of the transverse wavenumber. Therefore, only the radial direction of the aperture can be used for the speckle suppression mechanism. In this case, even using very long fibers and illumination from a wideband LD does not provide a solution for speckle-free laser projection since very large numerical apertures of the objective lens (several hundred times larger than the size of the human eye's pupil) will be needed to obtain speckle-free images. Thus, a modified method using both the radial and azimuthal directions of the aperture is required to create speckle-free images in the future research.

The dependence of the efficiency of speckle suppression on the optical parameters of the laser projector systems, especially the parameters of the multimode fiber, were obtained and discussed

in this paper. The experimental results were well explained by the theoretical analysis. Moreover, the developed theoretical model applies for a general multimode optical waveguide. Thus, this model is valid not only for multimode optical fibers, but also for other optical waveguides with different waveguide cross-section shapes.

Funding

Disclosures

The authors declare no conflicts of interest.

References

1. M. J. Weber, *Handbook of Lasers* (CRC, 2019).
2. Lan Xinju, *Laser Technology* (CRC, Edition II, 2018).
3. J. Landers, *Laser Science and Applications* (Willford, 2016).
4. K. V. Chellappan, E. Erden, and H. Urey, "Laser-based displays: a review," Appl. Opt. **49**(25), F79–F98 (2010).
5. S. K. Yun, J.-H. Song, I.-J. Yeo, Y. Victor, S.-D. An, H.-W. Park, H.-S. Yang, K.-B. Han, Y.-C. Lee, Y.-J. Choi, S.-H. Lee, M.-S. Oh, D.-H. Shin, J.-S. Kim, S.-W. Ryu, K.-Y. Oh, Y.-J. Ko, S.-K. Hong, C.-S. Park, S.-K. Yoon, J.-W. Jang, J.-H. Kyoung, Y.-S. Hong, C.-C. Kim, O.-K. Lim, A. Lapchuk, J.-K. Lee, D.-H. Park, S.-W. Shin, J.-C. Kang, S.-W. Lee, S.-K. Kim, G.-Y. Byun, S.-K. Oh, J.-S. Lee, Y.-N. Hwang, D.-W. Kim, K.-S. Woo, E.-J. Kim, C.-W. Park, C.-D. Go, Y.-J. Lee, B.-H. Kim, C.-H. Kim, D.-J. Kim, and J.-S. Park, "Spatial optical modulator (SOM): Samsung's light modulator for the next generation laser display," Proc. SPIE **6487**, 648710 (2007).
6. H. Song, H. Li, and X. Liu, "Studies on different primaries for a nearly ultimate gamut in a laser display," Opt. Express **26**(18), 23436–23448 (2018).
7. Y. Zhang, H. Dong, R. Wang, J. Duan, A. Shi, Q. Fang, and Y. Liu, "Demonstration of a home projector based on RGB semiconductor lasers," Appl. Opt. **51**(16), 3584–3589 (2012).
8. J. W. Goodman, *Speckle Phenomena in Optics: Theory and Applications* (Ben Roberts & Company, 2008).
9. G. Verschaffelt, S. Roelandt, Y. Meuret, W. Van den Broeck, K. Kilpi, B. Lievens, A. Jacobs, P. Janssens, and H. Thienpont, "Speckle disturbance limit in laser based cinema projection systems," Sci. Rep. **5**(1), 14105 (2015).
10. M. Kuwata, T. Sasagawa, K. Kojima, A. Michimori, H. Sugiura, Y. Hirano, and T. Endo, "Reducing speckle in laser displays with moving screen system," Journal of ITE **65**(2), 224–228 (2011).
11. F. Riechert, G. Bastian, and U. Lemme, "Laser speckle reduction via colloidal-dispersion-filled projection screens," Appl. Opt. **48**(19), 3742–3749 (2009).
12. J. I. Trisnadi, "Speckle contrast reduction in laser projection displays," Proc. SPIE **4657**, 131–137 (2002).
13. H. Matthias, "Wavelength beam-combined direct diode lasers of highest spatial brightness" (Konstanz, Univ., Diss., 2019). https://kops.uni-konstanz.de/handle/123456789/46706
14. S. Lowenthal and D. Joyeux, "Speckle removal by a slowly moving diffuser associated with a motionless diffuser," J. Opt. Soc. Am. **61**(7), 847–851 (1971).
15. S. Kubota and J. W. Goodman, "Very efficient speckle contrast reduction realized by moving diffuser device," Appl. Opt. **49**(23), 4385–4391 (2010).
16. L. Wang, T. Tschudi, T. Halldórsson, and P. R. Pétursson, "Speckle reduction in laser projection systems by diffractive optical elements," Appl. Opt. **37**(10), 1770–1775 (1998).
17. J. I. Trisnadi, "Hadamard speckle contrast reduction," Opt. Lett. **29**(1), 11–13 (2004).
18. V. Yurlov, A. Lapchuk, S.-K. Yun, J.-H. Song, and H.-S. Yang, "Speckle suppression in scanning laser display," Appl. Opt. **47**(2), 179–187 (2008).
19. A. Lapchuk, A. Kryuchyn, V. Petrov, and V. Klymenko, "Optimal speckle suppression in laser projectors using a single two-dimensional Barker code diffractive optical element," J. Opt. Soc. Am. A **30**(2), 227–232 (2013).
20. Z. Le, A. Lapchuk, I. Gorbov, Z. Lu, S. Yao, I. Kosyak, T. Kliuieva, Y. Guo, and O. Prygun, "Theory and experiments based on tracked moving flexible DOE loops for speckle suppression in compact laser projection," Opt. Laser. Eng. **124**(1), 105845 (2020).
21. A. Lapchuk, G. Pashkevich, O. Prygun, I. Kosyak, M. Fu, Z. Le, and A. Kryuchyn, "Very efficient speckle suppression in the entire visible range by one two-sided diffractive optical element," Appl. Opt. **56**(5), 1481–1488 (2017).
22. A. Lapchuk, O. Prygun, M. Fu, Z. Le, Q. Xiong, and A. Kryuchyn, "Dispersion of speckle suppression efficiency for binary DOE structures: spectral domain and coherent matrix approaches," Opt. Express **25**(13), 14575–14597 (2017).
23. S.-D. An, A. Lapchuk, V. Yurlov, J. H. Song, H. W. Park, J. W. Jang, W. C. Shin, S. Kargapoltsev, and S.-K. Yun, "Speckle suppression in laser display using several partially coherent beams," Opt. Express **17**(1), 92–103 (2009).
24. E. G. Rawson and J. W. Goodman, "Speckle in optical fibers," Proc. SPIE **0243**, 28–34 (1980).

25. J. G. Manni and J. W. Goodman, "Versatile method for achieving 1% speckle contrast in large-venue laser projection displays using a stationary multimode optical fiber," Opt. Express **20**(10), 11288–11315 (2012).
26. A. V. Prygun, Y. M. Morozov, T. Y. Kliuieva, Y. A. Borodin, and Z. C. Le, "Completely passive method of speckle reduction utilizing static multimode optical fibre and two-dimensional diffractive optical element," J. Mod. Opt. **66**(16), 1688–1694 (2019).
27. H. Weyl, "On the asymptotic distribution of eigenvalues," News from the Royal Society of Sciences in Göttingen, 110–117 (1911).
28. M. Abramovits and I. A. Stegan, *Handbook of Mathematical Functions with Formulas, Graphs and Mathematical Tables* (Dover, 1970).